Department of Space and Climate Physics

Department of Electronic and Electrical Engineering

Individual Project – Final Report

Measurements and Modelling of Bistatic Radar Signature of Wind Turbines

Submitted in partial fulfilment of the requirement for the award of the degree of

MSc – Space Science and Engineering

Submitted by

Veronika Yordanova

Supervisor

Hugh Griffiths

13.07.2012

Abstract

The aim of this project is to investigate if bistatic radars can be deployed to mitigate radar wind farm clutter and what is the best bistatic geometry to do so. To address this, the bistatic radar signature was studied using both experimental and simulated data and a way of mitigating this effect was considered. We measured the Doppler signature of a rotating fan with acoustic radar. The analysis proved that the results resemble measurements of a real turbine. Further examination on the Doppler shift for different radar geometries was performed by simulations. A minimised Doppler return was observed when the turbine was positioned on the line between the radar transmitter and receiver. With these set conditions, the effect of forward scattering was examined which enabled the target to acquire a zero Doppler signature. Analysis showed that Doppler return can be minimized by separating and arranging the transmitter and receiver of a bistatic radar system with an interfering target on an approximate line between them. Bistatic geometry could be applied for radar which has a wind farm in its range. These findings suggest that bistatic geometry could be used for radar ranges containing wind farms or other similar interferences, though further study of this geometry is required given the limited conditions of this analysis.

.

Contents

List of figures

List of tables

1. Introduction

In 2007 the European Union set a target that by 2020 20% of the countries' energy has to be obtained through renewable sources. This target is 15% for the United Kingdom. Since the UK is one of the windiest countries in Europe, wind power is currently one of the largest sources of renewable energy. The number of operating wind farms in England, Scotland, Wales and Northern Ireland is currently 343 with 3790 wind turbines installed. Since the beginning of 2012, there have been 47 approvals for construction of new wind farms and 34 refusals compared with 86 approvals and 85 rejections in 2011 [1]. One of the main reasons for the high rate of refusals and project cancellations is their potential impact or obstruction to low flying aircrafts near airports and radar.

The impact of wind farms on aviation is increasing as the size and number of their turbines increase. Although the greatest portion of unwanted echoes is due to the large radar cross section (RCS) from the stationary parts of the turbines, there are ways of filtering it. Another problem for radar comes from the fact that the Doppler signature of the blades can be easily confused with the Doppler return of an air target. This could disrupt the ability of the Air Traffic Control Services (ATC) to effectively operate airports and to maintain a safe environment. This is the reason enough to seek new solutions to the problem by improving or changing the design the turbines, radar systems, or both.

The motion of the blades of a wind turbine produces a Doppler shift which can be very similar to that of an airplane - the two signatures could interfere because they are contained within the same frequency bandwidth. There are various approaches to this problem. One is improving the algorithms used for detection and tracking of targets. Another is to build wind turbines from stealth materials. However, this approach could be prohibitively expensive as it is very difficult to make objects "stealthy" over various frequencies. Here we study third method which consists of deploying an additional radar receiver or, generally, bistatic radar geometry to mitigate wind farm clutter.

2. Theoretical background

The radar system performance is strongly dependant on the parameters and dimensions of the wind turbines inside the illuminating beam of the radar. In this section are presented briefly some conventional wind turbine characteristics and parameters which have been used for the analysis of their Doppler return for ATC radar. In addition, a brief introduction to the theory of radar systems is provided. The research was focused on studying a particular section of the radar systems, bistatic radar, but a comparison between conventional and widespread radar is useful to distinguish the advantages of each.

Wind turbine elements

The wind turbine elements are the rotor, nacelle, tower and foundation. There are different types of wind turbines, but the most widespread design is with 3 blade rotor on a horizontal axis and therefore this is the design used for this study. The blades of the rotor are attached to a nacelle, where the gear box, some electrical control systems and the generator are also placed. A tower holds up the rotor and nacelle, while the foundation prevents the wind turbine from falling. The materials used for building the tower are usually concrete or steel, while the blades are typically made of fibreglass. Radar Cross Section (RCS) is very much influenced by the material of the object reflecting the signal, but this is considered outside the scope of this study and is thus held constant in order to focus on geometric effects. The dimensions of wind turbines differ depending on their location and function. For this study, the most important parameter is the rotor diameter, since the motion of its blades gives the Doppler signature of interest for this study. A conventional turbine rotor diameter ranges up to 80m, although the

largest onshore turbines have a rotor diameter of 127m. The biggest offshore turbines can reach 120m in rotor diameter.

Figure 1 – Wind turbine model E-126 with a typical three blade rotor and horizontal axis [2]

Theory of radar systems

Radar definition and applications

Radar uses radio waves to detect and locate an object. The word radar comes from RAdio Detection And Ranging, but modern radar can also identify and classify targets or produce images of objects observed from a satellite. Radar works on the principle of sending a signal from its transmitter site, which then scatters off everything it encounters on its way and part of the energy is bounced toward a receiving antennae. The target echo is captured by the receiving antenna and processed to distinguish the relevant data from noise from the surrounding environment, such as sea, vegetation, static structures, etc. There are many applications of radar for both civilian and military purposes including air traffic control, weather forecasting, astronomy, navigation, collision avoidance, Earth observation and detection, tracking and guidance of weapon systems [3].

Doppler shift

This study is focused on analyzing the radar signature of a rotating turbine. The Doppler Effect is a change of the frequency of a wave to an observer when the source of the wave is moving either towards or away from it. In many radar applications there is relative movement between the target, being detected, and the radar system. By accounting for Doppler effect, both a target's location and relative velocity could be extracted from the target signal: when a target is moving either away from or

towards the radar, the phase of the received signal is constantly changing with respect to the movement of the object, and the rate of this change is relative to the velocity of the target. The Doppler shift in the signal's frequency is thus a rate of change of phase, or "phase lag":

$$f_D = -\frac{2}{\lambda}\frac{dr}{dt}$$

In this equation, f_D is the Doppler frequency, r is the distance between the radar and the target, t is time and λ is the signal's wavelength. The equation is negated because with an increase of path length (r), an increased phase lag is observed [4].

Moving Target Indicator

Another useful exploitation of the Doppler Effect is for rejecting of clutter based upon differing velocities of received signals. Moving Target Indicator (MTI) is a processor that is able to distinguish a moving target from clutter based on their different speeds. When an object is moving, sequential radar pulses will have changing phases while return from clutter will be the same. MTI systems with quadrature channel processing can take into account both the phase and amplitude outputs and have shown better performance than systems using phase shift or amplitude information independently. However, most of clutter exhibits Doppler spectrum and its suppression is harder to achieve. There are a number of research projects based on studying clutter and different methods of cancelling it. Clutter locking MTI is one solution which works by averaging the velocity of motion of the clutter (or radar platform). Another method is to average the measured phase change over several range bins, which provide information on the average velocity of the clutter. The averaged clutter velocity is then filtered.

Errors in target detection

Although there are a number of technologies developed to distinguish a target from clutter, there is always a chance of making errors, largely because target detection is a statistical process. Together with the possibility of detecting a target, there is a chance of having a false alarm (radar detects the presence of a target when there is no actual target) or missing a target (inability to detect the presence of a target when there is an actual target). For this reason, choosing a detection threshold is of great importance. In order to ignore as much of the noise as possible, a high threshold should be selected and thus the false alarm probability is minimised. However, if the threshold is too high, there is a possibility of missing a target. In the case of wind farms the main source of impacts on radar is that their rotors create intermitted clutter which can be let through the MTI filters and create track-like indications on the radar screen. This is why conventional ATC radar will not have the ability to separate the Doppler shift of turbines from a real target if there are wind farms returns interfering with returns from nearby flying aircrafts.

Bistatic radar

Most radar systems built and used currently are monostatic, although the first radar, built in 1904 [5] and its early successors were bistatic. Monostatic geometry is obtained when the transmitter and receiver are located near each other or use a single antenna. A bistatic radar system has its transmitter and receiver separated at a considerable distance. This makes its geometry very specific, and therefore some unique features are introduced which differ from the properties of the monostatic radar. Bistatic radar systems are still in use, but they perform specific tasks where a monostatic substitute is not feasible. Figure 5, also referred to as a bistatic triangle, shows the defining parameters of the bistatic geometry.

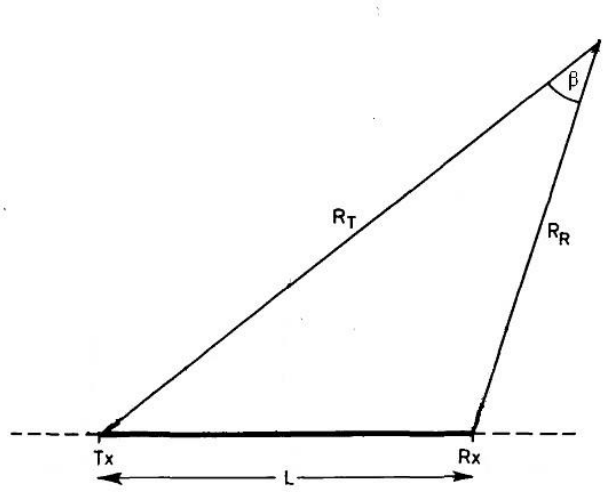

Figure 5 – Bistatic geometry [6]

The distance between the transmitter (T_x) and the receiver (R_x) is called the baseline (L). The angle between T_x, the target, and R_x is called the bistatic (also meaning cut or scattering) angle (β). This parameter is usually used to compare the performance between bistatic and monostatic radar. β/2 is called bistatic bisector. R_T is the distance that is travelled from the transmitted signal and R_R is the echo path of the scattered signal after bouncing off the target. Most of the advantages or problems associated with bistatic radar come from this geometry.

To understand bistatic radar signature, it is important to define some Doppler relationships for such geometry. In Willis's "Bistatic Radar" [7] a detailed study on this subject can be found. Some of his results are explained here since they will be needed for further analyses.

The definition of bistatic Doppler shift is the change of path length of the scattered signal with time, normalised by the wavelength of the signal:

$$f_B = \frac{1}{\lambda}\left[\frac{d}{dt}(R_T + R_R)\right]$$

In this equation, f_B stands for the bistatic Doppler frequency, λ is wavelength of the signal and $R_T + R_R$ represents the total path length that the signal covers.

With a stationary transmitter and receiver and a moving target, the bistatic Doppler shift is defined by (1):

$$f_B = \left(\frac{2V}{\lambda}\right) cos\delta cos\left(\frac{\beta}{2}\right) \quad (1)$$

Here V is the magnitude of the velocity vector of the target, δ stands for aspect angle of the target velocity vector with respect to the bistatic bisector, and β is the bistatic angle.

There are some special features of this equation when β and δ contain particular values:

- If β=0, then the bistatic geometry is reduced to monostatic with the transmitter and receiver at the bistatic bisector. The magnitude of the Doppler target return for monostatic radar is always greater than that from any bistatic radar configuration.

- For β=180 degrees, the configuration is called forward scatter and the Doppler shift is zero for any value of δ. This means that when the forward scatter effect is observed, the Doppler shift stays the same regardless of the velocity of the target.

- If $\delta = \pm 90°$, for all β, the Doppler shift is zero because the velocity vector is perpendicular to the bistatic bisector.

All these geometries are simulated and analysed further in the report.

3. Measurements

The purpose of this experiment was to create a realistic approximation of ATC or marine radar detecting Doppler returns in a minimized lab version. The equipment used for performing the measurements was an acoustic radar system and a fan. The MATLAB programming language was used for data processing and analysis. The experiment was performed in acoustics at ultrasound frequency.

Analysis of the Measurement

Data was collected in a lab experiment performed in UCL providing results on Doppler signature measurements. A schematic representation of the performed experiment is provided in Figure 9.

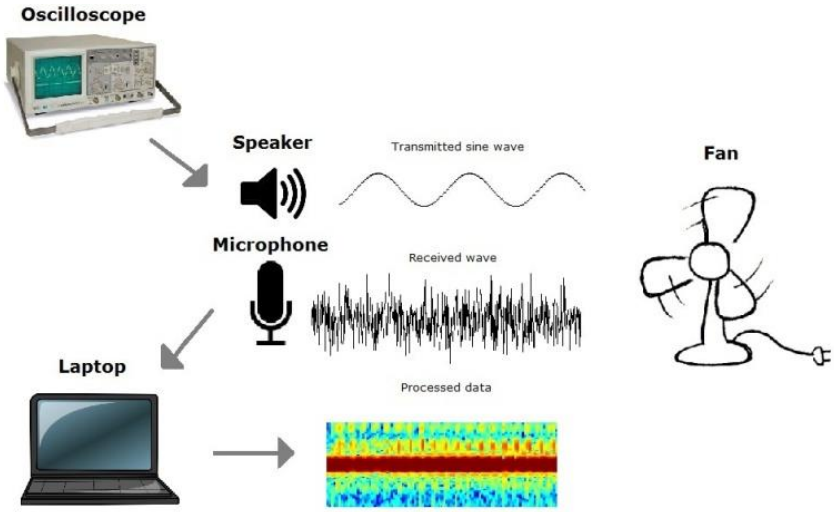

Figure 9 – Block diagram of the lab experiment with ultrasound acoustic radar

For this experiment, the signal parameters were set to amplitude $A = 0.2\ V$, pulse duration $t = 4\ s$ and frequency $f = 60\ kHz$. On the block diagram, the oscilloscope represents the hardware of the transmission channel: encompassing the software generation of the signal, its analogue conversion, and its amplification. This signal is emitted from a speaker, and upon reaching the interfering fan, parts of the signal are reflected back, resulting in a noise-like signal. This distortion is mainly caused by the propagation effects the environment has upon the signal. Also the Doppler shift from the rotation of the fan blades is added to the signal and it is the part in which our study is interested. The target echo is captured by receiving channel (represented by a microphone on the diagram), which records the signal,

amplifies it, and converts it back from an analogue input into a digital one. The data provided can then be processed by a computer algorithm to give a colour-coded diagram in which the motion of the blades is detected and is analysed.

Hardware

The equipment used was continuous-wave (CW) ultrasound acoustic radar which hardware is illustrated on figures 6 and 7.

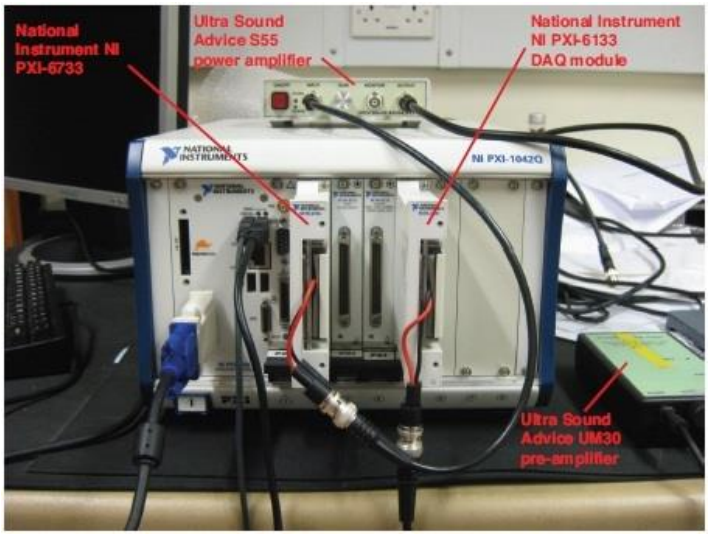

Figure 6 – Amplifiers and PXI platform [8]

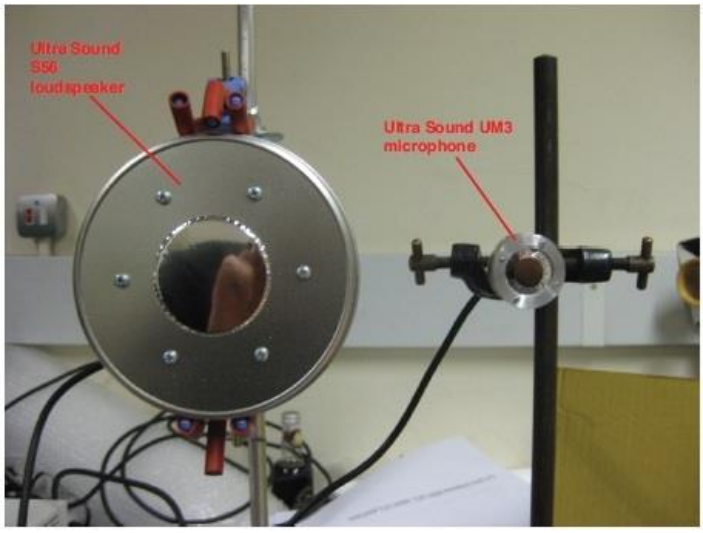

Figure 7 – Loudspeaker and Microphone [8]

The transmitter of the radar is composed of signal generator, power amplifier (PA) and loudspeaker. The receiver is comprised of a microphone, low noise preamplifier and data acquisition card (DAQ). The PC-based platform used to build the acoustic radar is a NI PXI-1042Q.

A transmission radar signal is first software generated and then converted to analogue with a NI PXI-6733 card. It is then amplified with an Ultra Sound Advice S55 PA and transmitted via an Ultra Sound Advice S56 loudspeaker. The maximum output voltage of the transmitter is 140V and its frequency can range between 18 and 300 kHz. The receiver channel starts with Ultra Sound Advice UM3 microphone, which is most sensitive for frequencies between 20 and 180 kHz. The signal is then amplified by an Ultra Sound Advice UM30 low noise preamplifier and digitized by an NI PXI-6133 DAQ card. [8]

Characteristics of the measurements

The fan used as a model wind turbine for this simulation has blades that are curved along their length and are connected to a hub attached to a pole. The pole is completely stationary while the hub is rotating with relatively little velocity. The RCS from the fan structure is not taken into account, so the material composition of the fan is not of large significance. .

The experiment was performed in a room with no wind or other meteorological effects to disrupt the measurements. The fan blades were rotated with constant speed in order to eliminate Doppler shift alterations normally caused by such changes. The RCS and the Doppler signature of this fan are also dependent on the yaw angle of the rotor with respect to the direction of the radar signal. As the RCS is not measured or simulated for this study, only theoretical assumptions and results from other similar experiments are to be provided. When the turbine is faced directly into the radar signal (a 0 degree yaw angle), a maximum RCS would be expected but minimal Doppler signature. When the turbine is sideways with respect to the radar signal (a 90 degree yaw angle), minimum RCS and maximum Doppler return should be observed. Figure 8 illustrates the yaw angle of a wind turbine in respect to radar for 0 and 90 degrees, with the point of view of the observer representing the point of view from the radar signal source. The turbine illustrated is not part of the equipment used but was used in another research project measuring Doppler signatures from micro turbines performed by QuinetiQ [9].

Figure 8 - Turbine faced at 0 and 90 degrees (respectively) to the radar

Short Time Fourier Transform (STFT)

The algorithm used for processing the data collected in the experiment is the Short Time Fourier Transform (STFT). This algorithm is adjusted to fit the parameters needed to interpret results from Doppler signature simulation of ATC radar. Its advantage is that it provides information on frequency variation with time, for which the Discrete Fourier Transform (DFT) is not suitable. The algorithm that is used to represent DFT in MATLAB is called Fast Fourier Transform (FFT) and Figure 10 shows the use of FFT on the measured signals from the ultrasound radar used for the lab experiment. The x-axis represents frequency in Hz x 10^4 a against the signal amplitude (shown on the y-axis) of the signals in dB. The transmitted and received signals are displayed (Top and bottom, respectively). The *60 kHz* frequency for both signals can be easily spotted in the peak of the graphs, but the small variation of the

Doppler signature which gives the information of the rotating blades, cannot be separated. This is why the change of the frequency spectrum has to be observed using time-frequency analysis, such as STFT.

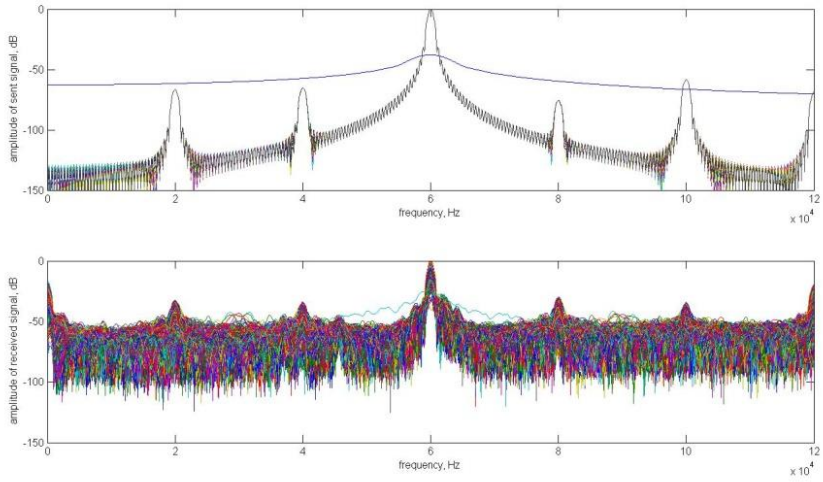

Figure 10 – FFT of transmitted and received signal using ultrasound radar

The data we receive form the radar is a CW signal but to compute the result this signal needs to be discrete. To obtain the discrete-time STFT we need a discrete signal *x[n]*. A continuous signal *x(t)* is digitized and sampled with sampling frequency F_s and thus:

$$x[n] = x(nT_s)$$

where *n* is the discrete time index and $T_s = 1/F_s$ is the sampling period. Then the STFT is defined as:

$$STFT_x[n,k] = \sum_{r=-\infty}^{+\infty} x[r]w[n-r]e^{-\frac{j2\pi rk}{N}}, \qquad k = 0,1,\dots,N-1$$

where *k* is the harmonic of the transform component, *w[n]* is a window function and *N* is the length of the STFT. The data is separated into pieces by multiplying the FFT of the signal with a windowing function. The length of the window is usually small, which allows the frequency in that time period to be considered stationary. The result of each piece is added to a matrix where the information of the magnitude and the phase of the signal are stored in frequency and time [8].

Measurements Results

The processed data with STFT of the lab experiment measurement can be seen on Figure 11, which shows the signal transmitted (top) and signal received.

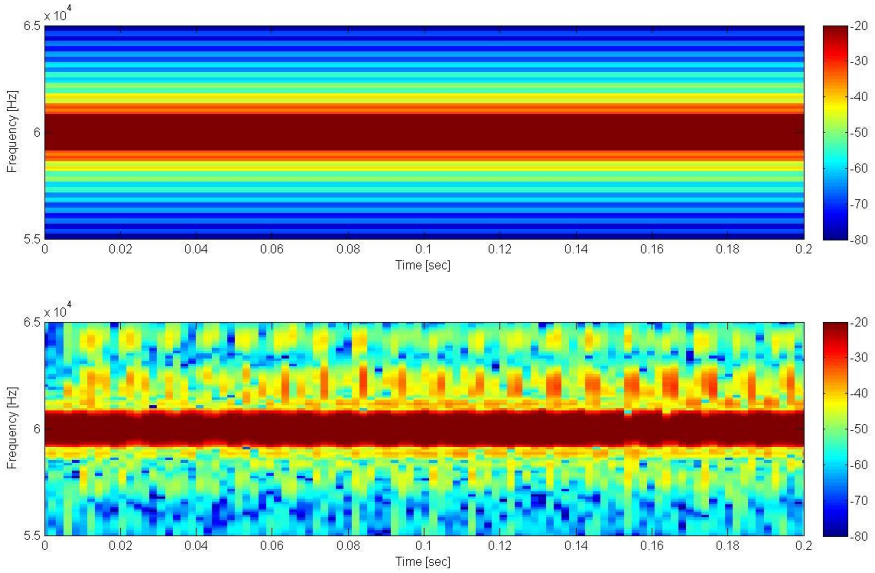

Figure 11 – STFT of transmitted (top) and received (bottom) signal using ultrasound acoustic radar at UCL

Magnitude of the signal

The colour legend in the right end of Figure 11 shows the scale of the signal magnitude. It shows the RCS of the returned echo due to the Doppler signature of the rotating blades. As can be seen, the scale ranges from -20 to -80 dB. This corresponds to serious attenuation and the strongest signal that is displayed is 100 times weaker than the one actually received. This is was due to the fact that the algorithm used did not compensate for the additional signal received directly from the transmitter, a consequence of locating the transmitter very close to the receiver. This inevitably causes the strong, direct signal to be received along with the signal reflected by the fan. This is an unwanted part of the data, so to avoid burying the echo that carries the fan's Doppler signature the graph shows signals from 100 to $100x10^6$ times weaker than the original.

Plots

The transmitted signal in Figure 11, formed at a frequency of *60 kHz*, is represented by a thick red line along the entire time period of the graph at $6x10^4$ Hz on the y-axis. There is no measureable noise or disturbance in this signal as it is software generated.

The bottom graph displays the STFT of the received signal. This image is very different from the top one, but still a thick red line is stretching horizontally at $6x10^4$ Hz on the y-axis. This is the interference in the receiver from the strong transmitting signal mentioned before. The consecutive red vertical lines represent the signature of the blades and as the time axis is in the small interval between *0* and *0.2 s* we can see the rapid rotation of the blades. As the transmitted sine wave is variably reflected by the fan blades, due to their movement, a Doppler shift is added to the *60 kHz* frequency. A relatively small change of around *0.5 kHz* is observed for the fastest moving parts of the blades.

Tradeoffs between time and frequency resolution

Since the measured Doppler shift is so small, the parameters for the STFT algorithm need to be chosen carefully so that a high resolution in frequency can be obtained. The length of the window function is responsible for the resolution of the signal. A large window increases the frequency resolution, but there are limitations to how much we can increase its size given that the time resolution depends on it as well. There is a trade off between time and frequency resolution. In order to obtain a good frequency resolution, the window length should be large because the process can be observed in more detail. But with too large a window, there may be too much information averaged to obtain an adequate time resolution. When decreasing this window, the opposite effect is observed, improving the resolution in time but deteriorating the frequency resolution. The length of the FFT in every window from the STFT is also responsible for the accuracy of the display of data in the selected window. The larger the FFT length, the more detailed is the data in the window.

Sampling time and frequency

Another parameter that is important when using a discrete time algorithm such as STFT is the sampling frequency F_s. This variable is responsible for defining the number of samples per unit of time in a continuous signal to make it discrete. Choosing the right sampling frequency will avoid aliasing, which distorts the original signal and makes it difficult to distinguish. The Nyquist theorem [10] states that the sampling frequency must be at least twice as big as the highest frequency of the signal being sampled. However, there is a limitation on how high the sampling frequency can be increased through the computational abilities of the processor used for running the algorithm. The sampling frequency defines the time between two samples, or "sampling period" (T_s) as they are reciprocal parameters.

In-depth analysis

The Doppler profile detailed on Figure 12 shows the change of the Doppler signature with the alternation of the velocity and the curvature of the blades in length. The positive values on the graph correspond to the components moving towards the radar and the negative values are components moving away from the radar. It is evident that the fronts of the blades give much greater signature than the backs, with negative Doppler response. For this reason, three positive elements are zoomed out from the graph so an in depth analysis could be done.

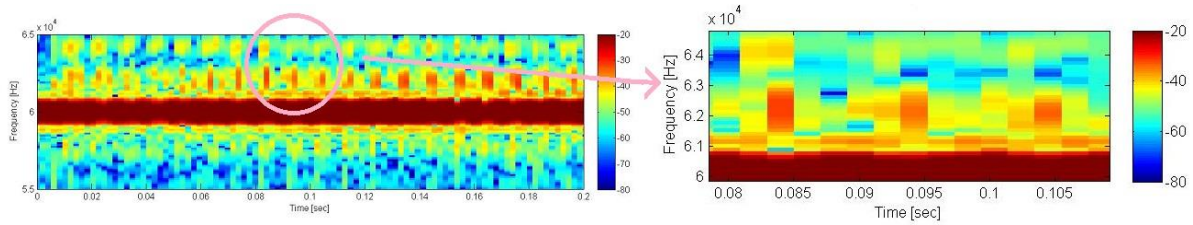

Figure 12 – In depth look at the Doppler return from rotating fan blades

As explained, the thick red line running horizontally through the graph is the signal leaked from the transmitter. It is hiding the zero Doppler returned from the static parts of the turbine. There could be small Doppler fluctuations around *60 kHz* (*0* Doppler shift) probably due to the rotation of the hub and the varying degrees at which the blades face the radar. The fluctuations around *61 kHz* are showing reflection of parts, moving with small velocity of the blades near the hub but still leaving the RCS large and relatively constant. With the corresponding increase of the Doppler return, the RCS diminishes and we can distinguish the separate blades. The highest visible RCS return is around *64 kHz* (a *4 kHz* Doppler shift from the basic signal) which is caused by the rotation of the tip of the blade. It produces the highest Doppler return because the tip speed of the blades is highest compared to the other parts of the fan. At *63 kHz* there seem to be almost *0* RCS in the graph, which could be caused by the specific design of the blades of the fan, which face the radar at an angle that minimizes the Doppler return. For

real rotating turbines, the relatively slow-moving interior blade sections could be filtered by MTI, but the tips of these blades produce a Doppler return that could be mistaken for a real target and have a potential negative impact that needs to be mitigated.

Comparison between acoustic radar and ATC radar

A comparison between an acoustic and ATC radar needs to be done. This will indicate whether or not the analyses made so far are realistic and can be applied to real data obtained from outdoor measurements. As discussed so far, the equipment used to replace ATC radar and a wind turbine were acoustic radar and a fan. There are some considerable distinctions between the lab model and real scenario resulting mostly from the frequencies at which the radar operates, bringing about the different speeds and propagation properties of the signals. However, measurements performed by acoustic radar in these tests are comparable to ATC radar detecting Doppler return from rotating turbines as can be seen by comparing their blade length to wavelength ratios. This is shown in Table 1 for acoustic radar, ATC radar and marine radar. The acoustic radar is working on a low frequency band, ranging in the tens of kHz, in this case *60 kHz*. In comparison, conventional ATC radar is using super high frequencies (around *3 GHz*), and marine radar works at around *9 GHz*. Both are in the electromagnetic (EM) spectrum. Propagation speeds of sound and EM waves in the air for standard atmospheric conditions are roughly *343m/s* and 3.10^8 *m/s* respectively. The wavelength in Table1 is given by the relation between speed and frequency. The next step is to give approximate values for the blades of the fan used for the measurements and a conventional wind turbine. The obtained ratio of blade length/wavelength differs by approximately one order of magnitude between the lab experiment and real scenario parameters. This number is reasonable to consider the results obtained from the measurements realistic and suggests that the experiment provides an effective model for investigation.

	Acoustic radar	**ATC**	**Marine radar**
Frequency, Hz	60 000	3 000 000 000	9 000 000 000
Speed, m/s	343	300 000 000	300 000 000
Wavelength, m	0,0057	0,1	0,0333
	Fan	**Wind Turbine**	
Blade length, m	0,1	20	
Ratio of Blade length/ Wavelength	17,49	200	600

Table 1 – Comparison between acoustic, ATC and marine radar

Another difference between using radar with acoustic and EM signals is the physics of their reflection from the target (fan and wind turbine blades respectively). The propagation characteristics of both signals are very distinct. When an acoustic wave reaches the fan blades, it makes them vibrate and a new acoustic wave is reflected from those vibrations. However, when EM wave is interacting with wind turbine blades, there is noise-like current propagating on their surface, which is scattered back. The effect of different polarization can be added to the EM signals properties, while the acoustic signal doesn't have such feature.

Comparison with Measurements for Real Turbines

After proving by calculations that the experiment performed are realistic, here is shown a comparison between the results obtained in the lab measuring Doppler return of rotating fan blades and measurements of real wind turbines.

Figure 13 shows the Doppler signature of a conventional turbine.

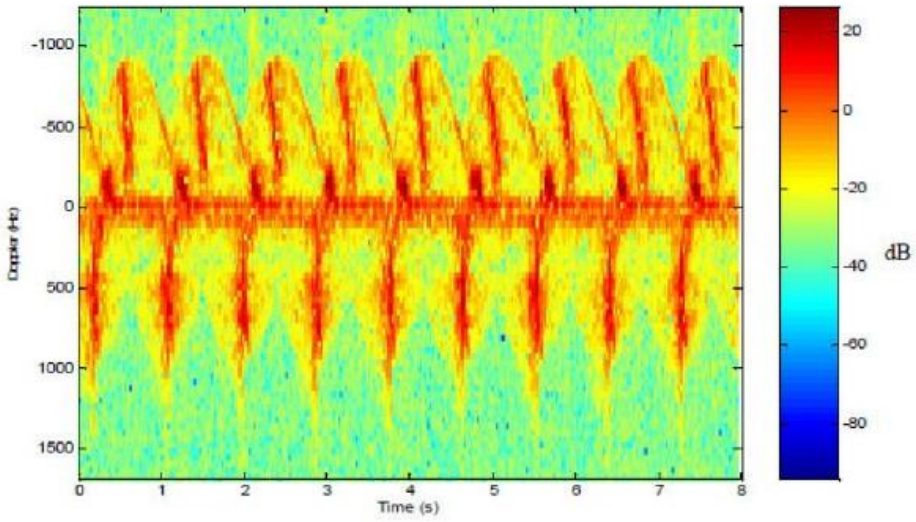

Figure 13 – Measurement of radar signature of a conventional wind turbine (FES W/14/00614/00/REP DTI PUB URN 03/1294, 2003) [11]

On this graph the carrier signal is extracted from the received signal so the Doppler signature is placed around the 0 frequency rather than around the carrier as in the graph from the measurements presented for this research. Another difference is that the positive and negative Doppler is reversed around the origin of the y-axis with comparison with the lab experiment results. The Doppler return from the turbine is around 5 times smaller than the one from the fan but this is likely due to the different frequency of the radar used and the blades speeds. Of course the designs of wind turbine blades differ greatly from the fan used and so the signature has some distinction, but important similarities can be seen. At the origin for both graphs there are 0 Doppler shifts, which correspond to stationary elements or something with a very low speed. With the increase of the Doppler, the signature of the separate blades becomes visible. Again the positive Doppler is higher than the negative, which means parts that are moving forward towards the radar have a greater signature than elements moving backwards from the radar. The tip of the blade in both cases produces the highest Doppler due to the highest velocity.

.

4. Simulations

The main purpose of the research is showing simulation of a Doppler signature for a conventional wind turbine. Modelling was done for several radar geometries so the effect of using bistatic radar in comparison with monostatic could be studied. However, the RCS for both geometries was considered the same and only the Doppler signatures were examined. In this section the results and some of the problems that aroused during the data processing are explained.

For conventional radar, there are various losses that are inevitable, although these can sometimes be mitigated or minimised. ATC and weather radar operate in the S frequency band. For such radar systems, some of the most significant losses are atmospheric loss and fluctuation loss, but they are not included in the simulation. Other losses which depend on radar design are also ignored, including those due to polarization of the EM signal, antenna rotation, and beam shape. There are multiple problems specific to the environment such as terrain clutter and multipath effects that are also not taken into account. The resulting model is a very simplistic one, focusing on the Doppler return from rotating points for a lossless system. However, it shows very clearly the difference made by the location of a receiver relative to a transmitter for a radar system. This is defined by the bistatic angle and so several geometries will be observed in this section.

MATLAB Code Analysis

Part of the code used to process measurements data of the performed lab experiment was also used for modelling the Doppler signature for typical ATC radar frequencies. However, there were many new calculations that needed to be done and old parameters adjusted for the new data sets in order to accurately represent the difference in frequencies between measurement and simulation, which was in the order of 50,000.

Wind Turbine Modelling

One of the new pieces of code added was for modelling a wind turbine. The challenge was that the blades of a real rotor rotate with different relative speed depending on their length – the centre of the turbine is effectively stationary, while the velocity increases to a maximum value at the tip. This is the reason different points create their own Doppler signature on the radar and this effect must be observed. However, graphs of this simulation became overloaded when too many points were displayed at the same time, and the results were inadequate for further analysis. For this reason only 3 points were considered at a time for each graph, giving the motion of the blades what looked like an intermittent motion when trying to show the gradual change of Doppler shift with increasing relative velocity along the radial direction. Further analysis was done for 3 points at the same diameter of the turbine, each representing a separate blade, and each of the tested radar geometry was represented with this hypothetical turbine.

Sampling Frequency

Another significant change in the code was introduced because the *3 GHz* frequency of ATC radar would normally require at least *6 GHz* sampling frequency (according to the Nyquist theorem [10], which exceeded the capabilities of the computer used for data processing. The solution was to extract the carrier signal from the received signal, since it did not provide any new information about the target. Thus only the signal containing the Doppler return was sampled and processed. Although the Doppler shift of the blades increased in radial direction, the frequency in the simulation did not exceed a few thousand Hertz. This was a considerable improvement on the computation speed of the data and no distortion or truncation was introduced to the final results. The sufficient sampling frequency F_s was chosen in the kHz range.

Calculating Time Delays

One of the key calculations for obtaining the radar signatures were the delay times of the signals. The time delay is the measure between transmission and reception of a signal. Consequently, if the detected target is further away from the radar, the delay time will be longer. Time delays can be used as an indirect measure of the distance for radar systems.

The way a delay time for a single point from the turbine was presented in the MATLAB code was by breaking each point into its 3 coordinates – x, y and z. Those coordinates were directly dependant on the time and the angular velocity for a given point. For a simpler representation the transmitter was considered to be located at a constant distance from the turbine so that the x coordinate was not changing in time. This simplification did not introduce any loss of data or inability to perform needed simulations, but allowed only the y and z coordinates to be calculated. The vector form of a random point from the turbine is shown in the equation:

$$a_n = \begin{pmatrix} x_n \\ y_n \\ z_n \end{pmatrix} = \begin{pmatrix} 0 \\ \sin(wt) \\ \cos(wt) \end{pmatrix}$$

where a_n is a random point from the wind turbine blade with w is the angular velocity of the blade, and t is the time.

The steps for estimating the delay time is shown in the following equations, where first, the distances are separately calculated from the transmitter and the receiver and then the total delay time is estimated:

$$D_T = \sqrt{(Tx - x_n)^2 + (Ty - y_n)^2 + (Tz - z_n)^2}$$

$$D_R = \sqrt{(Rx - x_n)^2 + (Ry - y_n)^2 + (Rz - z_n)^2}$$

$$\tau_n = \frac{D_T + D_R}{c}$$

D_T and D_R stand for distance from the transmitter and receiver, respectively. The delay time is abbreviated by τ_n, and $Tx\ Ty\ Tz$ and $Rx\ Ry\ Rz$ are the coordinates of the points chosen to represent the transmitter and receiver accordingly. The position of the point *n* on the turbine for which the calculations are being done is shown by $x_n\ y_n\ z_n$.

Results and analysis from simulation

Relation between tip velocity and Doppler shift

With the aid of the simulation performed, the relation between Doppler shift and radial increase of velocity for turbine blades was displayed and analysed. This was observed by modelling only one blade of the rotor and choosing different points between the centre and the tip of the blade. The dimensions of the examined rotor influenced the most the pattern of the observed parameters. For this reason, two separate examples were observed: one was displaying a conventional wind turbine – Suzlon s66/1250 [12] and another using the parameters of the biggest turbine built to date – Enercon E126 [1]. Figures 14 and 15 are photographs of these turbines.

Figure 14 – Wind turbine model Suzlon s66 with rotor diameter of 66m [12]

Figure 15 - Wind turbine model Enercon E-126 with rotor diameter of 126m [1]

To make a comparison between the two wind turbine types, the calculation of their blade velocities was made for equal wind speed *V=12 m/s*.

From the characteristics given by their manufacturers, [1], [12], the angular velocities and tip speed of both turbines were estimated.

The formulas used for calculations are:

$$w = 2\pi f = 2\pi \frac{v_r}{60} \quad (2)$$

$$v = wr = w\frac{d}{2} \quad (3)$$

where *w* stands for angular velocity and is measured in rad/s, *f* is frequency in Hz and v_r is the rotational speed of the blades which is given in revolutions per minute (rpm). In the second equation, the new parameter *v* represents the speed at the tip of the blade, measured in meters per second (m/s), *r* is the rotor radius and *d* is the rotor diameter, both measured in meters.

Results from calculations performed with equations (2) and (3) can be seen in Table 2. Both models were designed with variable rotational speed for their rotors, giving maximum and minimum values of this parameter in the table. Since the angular velocity is directly linked to the rotational speed, as shown in (3), there is a maximum and minimum values provided for it as well.

	Symbol	Dimensions	**Suzlon s66**		**Enercon E126**	
Rotor diameter	d	m	66,00		126,00	
Rotational speed (min and max)	v_r	rpm	13,50	20,30	5,00	11,70
Angular velocity (min and max)	w	rad/s	1,41	2,13	0,52	1,23
Tip speed	v	m/s	93,31	140,30	65,97	154,38

Table 2 – Calculation of wind turbines parameters

Here only the rotor diameter is taken into account, but the speed of the blades, which is related to the wind speed, is also influencing the Doppler shift. For the moment, most turbines are rotating with constant speed but the tendency is that the number of machines operating at variable speeds according to the wind speed change is increasing.

The simulated results show only monostatic radar configuration. Only graphs for the maximum tip speed from Table 2 were provided since this is where the Doppler shift is largest. Plots can be seen on Figure 16.

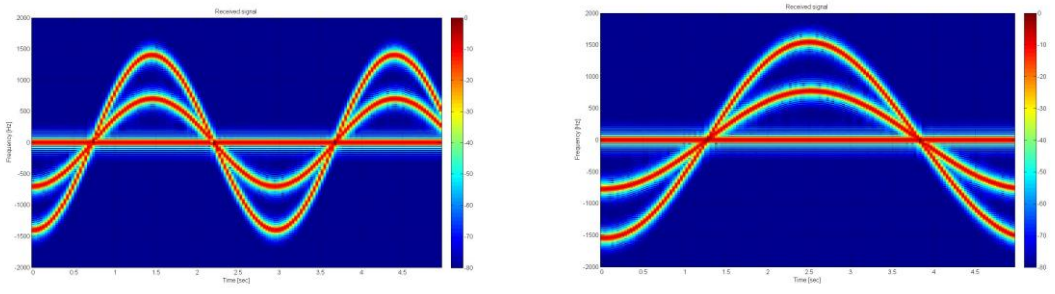

Figure 16 – Doppler signatures of a blade for conventional and large turbines (respectively)

The *0* frequency line is the point at the centre of the rotor. The angular velocity in this point is multiplied by *0* since it is stationary, resulting in no Doppler shift being produced by it. The middle line shows the Doppler return from a point in the middle of the blade, and the line with highest frequency is the tip blade

point. The difference between these graphs is that the turbine with the smaller rotor diameter produces almost twice as many shifts as compared to the larger wind turbine. This is because during the allocated simulation time of 5 s at the selected wind speed, the smaller sized blades have higher rotational speed and are able to make more revolutions than the bigger blades. The Doppler shift of the E-126 model is slightly larger, but both give shifts around 1.5 kHz.

Relation between radar geometry and Doppler shift

Radar geometry influences the Doppler returns from targets. When changing the location of the radar transmitter or receiver, the signal is sent or received at different angles. Hence, the objects from which the signal scatters have a new RCS relative to both the receiver and transmitter, but its study is out of the scope of this research. The Doppler shift also changes with alteration of the bistatic angle. For this paper several geometries are modelled and analyses of the effects they have on the Doppler return are provided.

In the following tables are summarised the results obtained from modelling of bistatic signature. Table 3 has data for the case in which the transmitter of the radar is facing the wind turbine sideways (at a 90 degree yaw angle). The receiver's position is then changed so that geometries of 0, 45, 90, 125 and 180 degrees are obtained. Angles, greater than 180 degrees, do not provide new information, as they negate the results seen with angles between 0 and 180 degrees. Table 3 shows the Doppler return from the simulated bistatic angles. Some of the graphs that show specific features of the radar geometry are shown and analysed and others are only accounted in the tables with their peak Doppler shift.

Bistatic angle	f, Hz
$\beta = 0°$	3900
$\beta = 45°$	2600
$\beta = 90°$	1900
$\beta = 125°$	500
$\beta = 180°$	0

Table 3 – Results from simulations for transmitter facing a wind turbine at 90 degrees yaw angle and different bistatic angles

As expected from equation (1), for $\beta = 0°$, which corresponds to monostatic geometry, the Doppler shift is greatest. With an increasing bistatic angle, the Doppler return decreases until it reaches 0 for $\beta = 180°$. Figure 17 illustrates Doppler signatures of the two cases – monostatic and forward scatter.

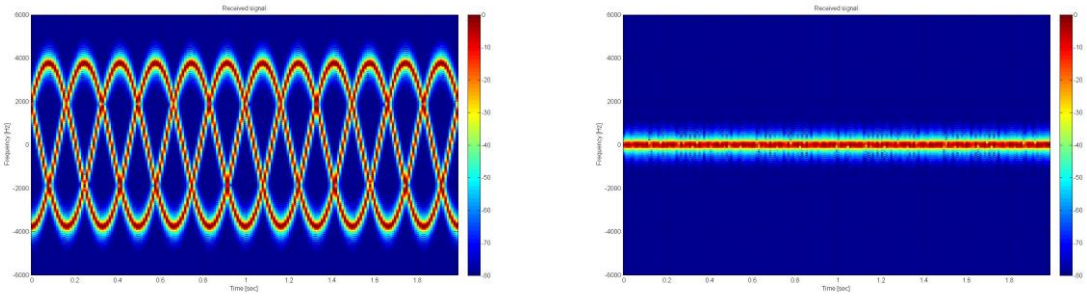

Figure 17 – Doppler signature for monostatic geometry and forward scatter (respectively) with transmitter facing a wind turbine sideways

The forward scatter effect in radar systems follows Babinet's principle from optics which suggests that the scattering from an opaque body is the same as from a hole of the same size and shape as that body. Applying this for radar systems means that a target would be easily detectable. However, if the target is on the baseline between the transmitter and receiver, there would be no range or Doppler information for it. This effect can be observed in the above graph.

Table 4 has data for the case when the transmitter of the radar is facing the wind turbine at the front (at 0 degrees yaw angle). Again different geometries have been simulated and Doppler shifts for bistatic angle at 0, 45, 90, 125 and 180 degrees are shown.

Bistatic angle	f, Hz
$\beta = 0°$	0
$\beta = 45°$	1200
$\beta = 90°$	1900
$\beta = 125°$	1200
$\beta = 180°$	0

Table 4 - Results from simulations for transmitter facing a wind turbine at 0 degrees yaw angle and different bistatic angles

The results for this configuration show that the Doppler shift increases with as the bistatic angle approaches 90. Equation (1) was defined for the case when the transmitter and receiver of the radar are stationary and the target is moving as in this simulation. The monostatic geometry here gives no Doppler shift because the target velocity aspect angle, δ, is pointing down the bistatic bisector. For $\beta = 180°$, the Doppler shift is also zero due to the forward scatter effect.

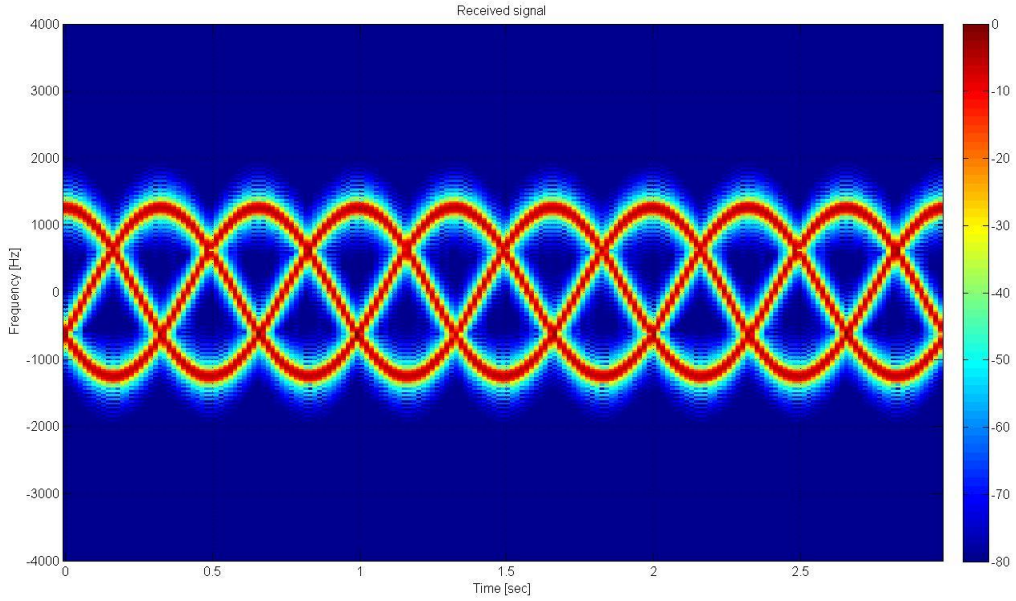

Figure 18 - Doppler signature for bistatic geometry with a bistatic angle of 90 degrees and transmitter facing a wind turbine at the front

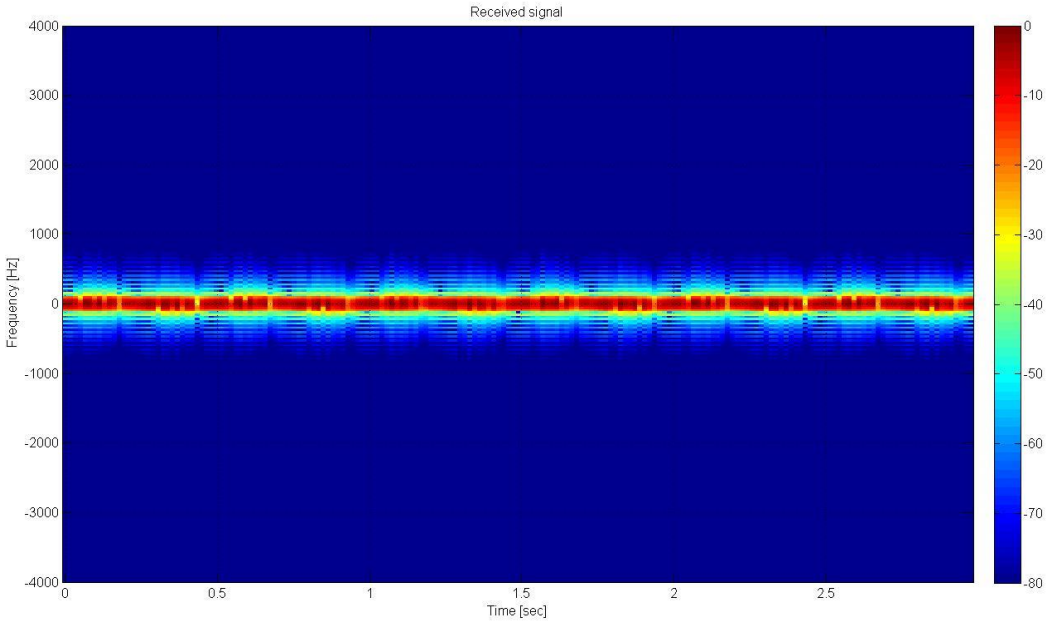

Figure 19 - Doppler signature for monostatic geometry and forward scatter with transmitter facing a wind turbine at the front

Table 5 has data for the case when the transmitter of the radar is facing the wind turbine at 45 degrees yaw angle. Again different geometries have been simulated and Doppler shifts for bistatic angle at 0, 45, 90, 125 and 180 degrees are shown.

Bistatic angle	f, Hz
$\beta = 0°$	2900
$\beta = 45°$	1400
$\beta = 90°$	0
$\beta = 125°$	500
$\beta = 180°$	0

Table 5 - Results from simulations for transmitter facing a wind turbine at 45 degrees yaw angle and different bistatic angles

For this configuration of the transmitter, the monostatic signature at $\beta = 0°$ is the largest compared to any bistatic. The 0 Doppler signature at $\beta = 90°$ is because the aspect angle of the velocity vector is perpendicular to the bistatic bisector. The same effect was observed for monostatic geometry with wind turbine at 0 degrees yaw angle. The forward scatter effect is present for $\beta = 180°$ and the Doppler signature was minimal.

5. Conclusion

Measurement results and simulated data provide a study on the effect the bistatic radar geometry has over the Doppler signature of wind turbines. The potential impact of wind farms on radar was investigated and a way of mitigating this was suggested. In a lab experiment, with an acoustic radar system and a fan, data was collected for the Doppler signature of the fan's rotating blades. The data obtained in ultrasound frequency was compared to data from measurements in radio frequency of wind turbine. The observed measurements proved to be a realistic approximation to real data. For further analysis of the Doppler signature, simulations were performed for ATC radar frequencies. This imposed the need of changing the algorithm used for data processing with parameters suitable for processing radio frequency signals. The relation between the tip speed velocity and the Doppler signature of a wind turbine was studied for different rotor diameters. It showed the dependence of the large blades with high speed to the increase of their Doppler returns. A way of mitigating the effect of the Doppler signature was searched by varying the geometry of a bistatic radar system. There were several cases observed when minimal Doppler frequency was detected: monostatic radar geometry when a wind turbine was facing it sideways and bistatic configuration with β= 90° with wind turbine facing the transmitter at 45° yaw angle. Those were not considered a good solution to the studied problem. Since there is usually a yaw mechanism in the rotor, which enables the turbine to change the angle it is facing the wind, the zero Doppler condition would not always be fulfilled. A third case was forward scatter. This effect was observed for any yaw angle between the transmitter and the turbine for bistatic angle of 180°. This bistatic geometry could be used for solving the problem of radars not being able to detect targets near wind farms.

6. Acknowledgement

I would like to thank Professor Hugh Griffiths for his time and help during the course of this research and Professor Alessio Balleri for the patience he had guiding me throughout all my work.

7. References

[1] http://www.bwea.com

[2] http://www.enercon.de/en-en/66.htm

[3] Kingsley, S., Quegan, S., "Understanding radar systems", McGRAW-HILL Book Company, 1992

[4] Griffiths H., Lectures on Radar systems, UCL, 2012

[5] Willis, N.J., Griffiths, H.D., "Advances in Bistatic Radar", SciTech Publishing, Inc, 2007

[6] Jackson, M.C.,"The Geometry of Bistatic Radar Systems", IEE Proc., 13397) Pt. F, 604-612, December 1986.

[7] Willis, N.J., "Bistatic Radar", Technology Service Corporation, Silver Spring, MD, 1995

[8] Lischi, S., 'Human recognition and motion classification by acoustic micro-Doppler signatures', 2011

[9] New, C., Moldau, S., "Study into the radar impact of a Micro turbine", QINETIQ/EMEA/TS/TR0707953/1.0, November 2007

[10] Person, J., "Basic Communication Theory", Prentice Hall, 1992

[11] Griffiths, H.D., Ohya, Y., Balleri, A., Tong, K., Al-armaghany, A. Matsuura, T. and Karasudani., T., 'Measurement and analysis of the radar signature of a new type of wind turbine', CIE International Radar Conference RADAR 2011, Chengdu, Vol. I, pp837–840, 24–27 October 2011.

[12] http://www.suzlon.com/products/l2.aspx?l1=2&l2=7

[13] Mahafza, B., Elsherbeni, A., 'MATLAB Simulations for radar systems design', Chapman and Hall, USA, 2004